https://doi.org/10.5194/egusphere-2026-4005
Preprint. Discussion started: 24 July 2026

Assessing and reducing dry-season water-scarcity risk on a tourism-exposed small island: a multi-source water-balance and robust-optimisation framework for Si Chang Island, Thailand

Uma Seeboonruang[1], Pinit Tanachaichoksirikun[1], Virun Chulkaivalsucharit[1], Jutamas Srisuk[2], Uba Sirikaew[1], Mongkol Prasitkumpein[3], Walter Chen[4]

[1]Department of Civil Engineering, School of Engineering, King Mongkut's Institute of Technology Ladkrabang, Bangkok, 10520, Thailand
[2]Department of Engineering, King Mongkut's Institute of Technology Ladkrabang Prince of Chumphon Campus, Chumphon, 86160, Thailand
[3]Water Management Division, Provincial Waterworks Authority (PWA) Regional Office 1, Chonburi, 20000, Thailand
[4]Department of Civil Engineering, National Taipei University of Technology, Taipei 10608, Taiwan

Correspondence to: Pinit Tanachaichoksirikun (pinit.ta@kmitl.ac.th)

Abstract. Dry-season freshwater scarcity is a recurrent hazard on small tropical islands, where seasonal rainfall, limited storage and tourism-driven demand coincide. We assess and reduce this risk for Si Chang Island, Thailand, with an integrated framework that resolves inter-month storage carry-over across coupled sources. Connected catchment is estimated from a land-use layer and satellite imagery, separating rooftop harvesting to household cisterns from watershed runoff to the reservoir–pond–bank system, while tourism demand enters through an equivalent-resident formulation. Supply reliability is quantified with reliability–resilience–vulnerability metrics under a downscaled CMIP5 ensemble, from which RCP4.5 is selected by bias screening. A mixed-integer optimisation, extended to a two-stage robust formulation, sizes capacity against stochastic dry years. Rooftop harvesting is the dominant source, and the present system is reliable but limited by small cistern capacity; under projected demand a structural annual deficit renders the island supply- rather than storage-limited, so additional storage alone cannot secure supply and harvestable catchment must expand. Critically, a design optimised on mean rainfall delivers markedly lower reliability under realistic variability, and drought-robust sizing requires substantially more catchment. The framework yields transferable, drought-robust design targets for small islands.

1 Introduction

Dry-season freshwater scarcity is a recurrent hazard on small tropical islands (Wohl et al., 2012). Limited catchment area, small surface storage, thin and salinisation-prone aquifers, and isolation from mainland networks leave island supply highly exposed, and these constraints are tightening as climate change shifts rainfall, raises sea level and intensifies extremes (Holding and Allen, 2016; Imig et al., 2025; Seeboonruang et al., 2026; White and Falkland, 2010). The defining difficulty is temporal: rainfall and runoff swing sharply between seasons, so wet-season abundance must be carried over to a dry season in which demand is highest (Ault, 2016). The result is recurrent, often unplanned, shortage, with most Small Island Developing States

https://doi.org/10.5194/egusphere-2026-4005
Preprint. Discussion started: 24 July 2026

below the 1,700 m³ per-capita water-stress threshold; tellingly, some islands hold adequate water in aggregate yet cannot deploy it because storage, conveyance and the ability to quantify their own resources are lacking (Global Center on Adaptation, 2025; Intergovernmental Panel on Climate Change, 2021; Parker et al., 2023). Tourism intensifies the mismatch from the demand side, since peak-season visitors and seasonal labour multiply the resident population and a visitor consumes more water per day than a resident, so the demand peak coincides with the supply trough (Gössling et al., 2012; Pérez et al., 2020; Srisuk et al., 2026).

Recent research underscores a global trend toward greater precipitation variability and heightened extremes. Mirzaei et al. (2025) highlighted significant intensification of extreme precipitation events, stressing the importance of adaptive infrastructure to manage these hydrological changes effectively. Similarly, Fiaz et al. (2025) noted that alterations in the South Asian monsoon, characterized by increased unpredictability, present significant water management challenges for islands that rely heavily on seasonal rainfall to sustain year-round water supply. The mismatch between seasonal rainfall availability and actual water demand presents another critical vulnerability for island communities. While rainwater harvesting is widely promoted as a resilience strategy, its effectiveness heavily depends on infrastructural, institutional, and policy-level adaptations. Haider et al. (2023) emphasized that capturing increased seasonal rainfall could significantly alleviate water deficits, yet its success is contingent upon proactive investment in adequate catchment and storage infrastructure. Likewise, Mashhadi Ali et al. (2017) indicated that inflexible water management strategies exacerbate temporary shortages, underscoring the need for adaptive management approaches to maintain stable water supply under fluctuating rainfall conditions. Furthermore, broader ecological and socio-economic vulnerabilities compound these physical stressors. For instance, ecological degradation and coastal infrastructure vulnerabilities further heighten islands' sensitivity to climate impacts (Sealey, 2024). Socio-economic dynamics such as population density, behaviour, and economic dependency also shape water vulnerability and adaptive capacity, necessitating a holistic approach to resilience-building that integrates both biophysical and socio-economic dimensions (Birawida et al., 2021; Chen and Tang, 2024).

Most island water research nonetheless centres on groundwater — freshwater-lens dynamics, recharge and saltwater intrusion under over-pumping and sea-level rise — or on desalination, which is energy-intensive and can itself promote intrusion. Islands whose principal input is rainfall captured in surface storage, where seasonal storage and harvesting rather than lens management govern security, are comparatively under-studied. For such systems, rainwater harvesting (RWH) is central, and a substantial literature sizes storage for reliability and cost by water-balance simulation or by linear and mixed-integer programming (Okoye et al., 2015; Semaan et al., 2020). A recurring but under-exploited result is that reliability is governed jointly by storage and catchment — beyond a point, enlarging tanks yields diminishing returns while additional catchment can substitute for storage (Semaan et al., 2020; Thomas and Martinson, 2007). Yet most studies size a single source under a stationary climate, and island analyses that resolve rooftop harvesting, reservoirs, groundwater and imports within one temporal balance remain scarce (Tanachaichoksirikun, 2026).

Two further elements are typically missing. Transient tourism demand, although large and counter-cyclical, is usually treated as an external stressor rather than as a modelled term of the water balance (Gössling, 2001; Gössling et al., 2012). And although

https://doi.org/10.5194/egusphere-2026-4005
Preprint. Discussion started: 24 July 2026

projecting future supply requires downscaled, bias-corrected climate output — simple water-balance reservoir models forced by CMIP (Intergovernmental Panel on Climate Change, 2023) ensembles being a transparent route that consistently shows multi-year droughts, not mean shifts alone, drive failures (Holmes et al., 2022) — the explicit screening of general circulation models for engineering-appropriate scenarios is rarely formalised, and the migration from CMIP5/RCP to CMIP6/SSP remains uneven (Dash et al., 2023; Guo et al., 2022).

Finally, performance and design are seldom brought together for these systems. The reliability–resilience–vulnerability (RRV) framework remains the standard for judging supply performance, and design methods span deterministic optimisation through two-stage stochastic and robust formulations that size capacity against uncertain futures (Hashimoto et al., 1982), with the recurring lesson that systems optimised for mean conditions can be fragile under variability (Asefa et al., 2014; Beh et al., 2017; Herman et al., 2015; Ortiz-Partida et al., 2019). These methods are mature for large basins and networks but are seldom applied to small-island, multi-source village systems at monthly resolution with an explicitly measured harvestable inflow.

Each ingredient therefore exists in isolation, but they have not been combined. We are not aware of a study that, for a tourism-exposed, fractured-rock small island, closes a physically consistent monthly multi-source water balance with storage carry-over, drives it with a measured rather than assumed harvestable catchment and an embedded transient-demand term, and sizes capacity through optimisation stress-tested against dry-year and multi-year-drought variability. Integrating these elements for Si Chang Island, Thailand, this study contributes: (i) a measured estimate of connected harvestable catchment from a land-use layer and satellite imagery, separating rooftop harvesting (to cisterns) from watershed runoff (to the reservoir–pond–bank system); (ii) a two-subsystem monthly water balance with storage carry-over and an embedded tourism-demand term, evaluated through RRV metrics under a downscaled CMIP5 ensemble with formal bias screening; (iii) a mixed-integer optimisation, extended to a two-stage robust formulation, that sizes least-infrastructure capacity against stochastic dry years; and (iv) transferable findings, notably that under projected demand the system is supply- rather than storage-limited and that mean-climate design substantially overstates achievable reliability.

2 Study area and input data

2.1 Location and land use

Si Chang Island (approx. 13°09′ N, 100°49′ E) lies in the inner Gulf of Thailand about 36 km from Chonburi and spans a mapped land area of 6.45 km². Its terrain is predominantly mountainous and rocky — roughly 80 % rock — rising to the King Chulalongkorn Mountain Peak (≈192 m) in the north, and its elevation is unevenly distributed: about 67 % of the island lies below 50 m, 26 % between 50 and 100 m, 6 % between 100 and 150 m, and only 1 % above 150 m (Figure 1). This combination of limited flat land and geographic isolation constrains both groundwater development and freshwater management, and underlies the island's reliance on rainfall capture. The island supports about 4,522 registered residents in 2,270 households (Department of Provincial Administration, Thailand, 2024), and its building roofs fall predominantly within the City/Town/Commercial class (U1 = 0.964 km²), which sets the denominator for the roof-area fraction (Table 1).

https://doi.org/10.5194/egusphere-2026-4005
Preprint. Discussion started: 24 July 2026

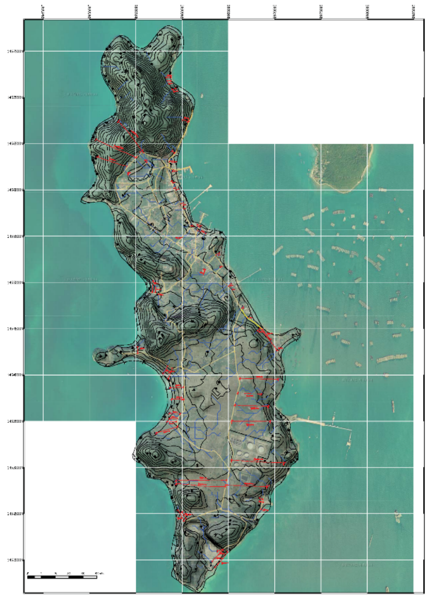

Figure 1: Location of Si Chang Island. (modified from Seeboonruang et al. 2026, base data: Royal Thai Survey Department (RTSD)

Table 1. Measured land use of Si Chang Island from the project GIS layer (Land Development Department classification).

Land-use class	**Code**	**Area (m²)**	**Area (km²)**
Deciduous forest	F2	4,449,961	4.450
City, town, commercial	U1	963,663	0.964
Industrial land	U5	419,024	0.419
Institutional land	U3	164,130	0.164
Communication / utility	U4	56,486	0.056
Mine, pit	M3	120,669	0.121
Natural water body	W1	244,701	0.245
Artificial water body (reservoir, ponds)	W2	34,335	0.034
Built-up total (U1+U3+U4+U5)	U	1,603,303	1.603

https://doi.org/10.5194/egusphere-2026-4005
Preprint. Discussion started: 24 July 2026

2.2 Climate, rainfall and runoff

Monthly rainfall is derived from ten years for the period 2012–2021 of Thai Meteorological Department records (TMD, 2021). The regime is strongly seasonal: a wet season from May to October contributes the bulk of the ≈1,195 mm annual total (peaking at 242 mm in September), while December–February is very dry (December ≈10 mm) (Figure 2). Watershed runoff to the reservoir is estimated from rainfall, the contributing watershed area (A_{ws} = 268,878 m²) and a weighted runoff coefficient (C_{ws} = 0.31), giving an annual reservoir inflow of about 140,020 m³.

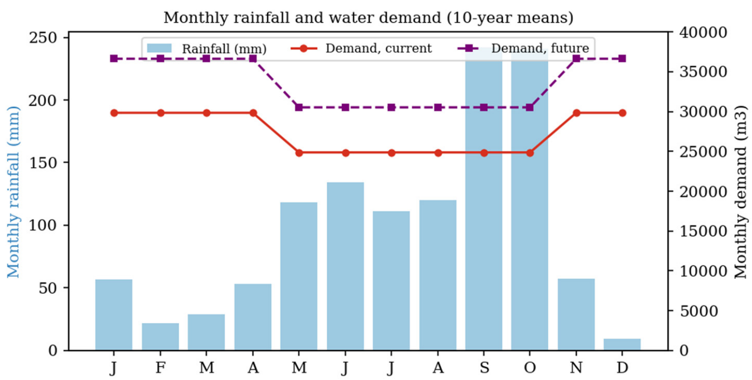

Figure 2: Monthly rainfall (10-year mean) and monthly water demand (current and future scenarios).

2.3 Storage infrastructure, groundwater, and external supply

Freshwater is held in four physically distinct stores (Figure 3 and Table 2). The main reservoir (83,000 m³) and four natural ponds (29,744 m³) are fed by watershed runoff; a capsule water bank (3,400 m³) is filled by pumping from the ponds, which lowers the pond level and pressure so that subsequent rainfall refills the ponds — the bank therefore effectively extends the usable capacity of the pond system. The main-system capacity used in the balance is 83,000 + 29,744 + 3,400 = 116,144 m³; the cistern subsystem is 5,650 m³. Separately, distributed under-house cisterns (5,650 m³ in total) store rooftop rainwater at the household level. Sustainable groundwater is limited to about 1,440 m³ per month by the fractured-rock setting, and barged Provincial Waterworks Authority (PWA) water can be delivered at up to about 1,500 m³ per day.

https://doi.org/10.5194/egusphere-2026-4005
Preprint. Discussion started: 24 July 2026

Figure 3: Water bank and Natural Water Pond in Si Chang Island

Table 2. Water-storage and supply inventory.

Store	Source	Capacity (m³)	Role in model
Main reservoir	Watershed runoff	83,000	Main system
Natural ponds (×4)	Watershed runoff	29,744	Main system
Water bank	Pumped from ponds	3,400	Extends usable pond capacity
Household cisterns	Rooftop harvest	5,650	Cistern subsystem
Groundwater	Aquifer	≤1,440 / month	Supplementary source
PWA import	Mainland (barged)	≤1,500 / day	External backstop

2.4 Population and water demand

Tourism is a significant driver of fluctuating water demand on Si Chang Island, largely because of the high proportion of short-term and unregistered visitors. A visitor survey (Nusara, 2021) found that most tourists do not stay overnight: 55.39 % were one-day visitors, 42.61 % stayed one to three days, and only 2.01 % stayed four to six days. To translate this transient population into a demand equivalent, we estimate the Equivalent Monthly Visitors (EMV), which combines the annual number of visitors with their average length of stay — taken as 1, 2 and 5 days for the three categories, respectively.

Water demand reflects both residents and the transient tourism population. From a visitor survey, annual visitors V are split into fractions P_k staying L_k days; the equivalent resident-persons added by visitors per month are

$$EMV = V \times \frac{(P_1 \times 1 + P_2 \times 2 + P_3 \times 5)}{12 \times 30} \quad (1)$$

https://doi.org/10.5194/egusphere-2026-4005
Preprint. Discussion started: 24 July 2026

which for V ≈ 600,000 yr^{-1} and stays of 1, 2 and 5 days (fractions 0.554, 0.426 and 0.020) gives EMV ≈ 2,511 persons. Adding transient labour (taken as ≈50 % of EMV, ≈1,256 persons) to the residents yields a current water-using population of $P_{tot} \approx$ 4,522 + 2,511 + 1,256 ≈ 8,289 persons; under projected population and tourism growth this rises to ≈10,173. Monthly demand is

$$D(t) = P_{tot} w_p(t) d(t) \tag{2}$$

with per-capita use $w_p(t)$ of 0.12 m^3 d^{-1} in the dry season and 0.10 m^3 d^{-1} in the wet season and d(t) the number of days in the month. The resulting monthly demand (Table 3) is 24,867–29,840 m^3 at present and 30,519–36,623 m^3 in future — slightly higher in the dry season, compounding the seasonal mismatch.

Table 3. Water-using population and monthly/annual demand. The current total is the sum of registered residents, equivalent visitors (EMV) and transient labour; the future total follows the demographic and tourism projection.

Population scenario	Residents	EMV (visitors)	Labour	Total P_{tot}	Demand, dry (m^3 mo^{-1})	Demand, wet (m^3 mo^{-1})	Annual demand (m^3)
Current	4,522	2,511	1,256	8,289	29,840	24,867	328,244
Future (projected)	—	—	—	10,173	36,623	30,519	402,852

2.5 Roof catchment estimation

Because connected roof area is not mapped directly, it is estimated by two independent methods. The primary (household) method scales the registered-household count by a building factor of ≈1.2 (to include commercial, resort, institutional and utility structures) and a mean roof footprint of 90 m^2 (range 70–110 m^2),

$$A_{roof} = N_b \bar{f}_{roof} \tag{3}$$

giving $A_{roof} \approx 2.45 \times 10^5$ m^2 (1.9–3.0 × 10^5 m^2). As a cross-check, roofs were classified from high-resolution Google Earth (Maxar/Airbus; pixel size 0.93 m) covering the entire eastern settlement (Figure 4). A conservative classifier capturing only unambiguous bright roofs returns ≈4.1 ha as a hard lower bound, and a permissive classifier that also admits dry-soil pixels returns ≈30.7 ha as an upper bound; the household estimate (24.5 ha) lies centrally within these bounds, and the implied roof fraction of the U1 area (≈0.25) is consistent with dense low-rise settlements. Direct GIS footprint digitisation is identified as a route to tighter (±5 %) estimates.

https://doi.org/10.5194/egusphere-2026-4005
Preprint. Discussion started: 24 July 2026

Figure 4. Satellite basis for roof-catchment estimation bounding the roof area. Imagery © Maxar Technologies / Airbus via Google Earth.

3 Methods

The modelling chain converts the input data into a monthly water balance, evaluates supply reliability under climate scenarios, and sizes capacity by optimisation, first deterministically and then robustly against stochastic dry years (Figure 5).

https://doi.org/10.5194/egusphere-2026-4005
Preprint. Discussion started: 24 July 2026

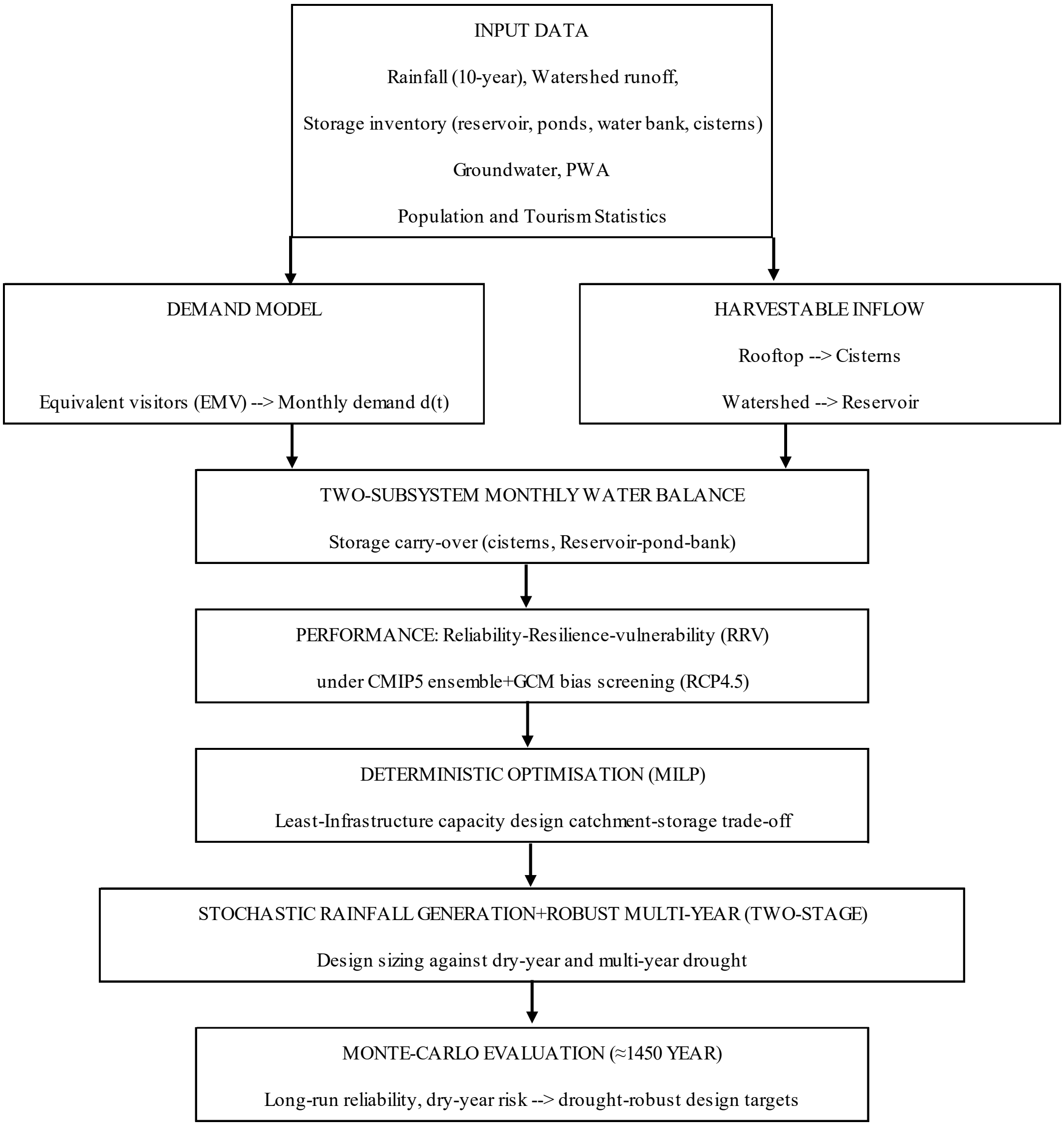

Figure 5. Methodology flow chart, from input data through the two-subsystem water balance and RRV evaluation to deterministic and robust capacity design.

https://doi.org/10.5194/egusphere-2026-4005
Preprint. Discussion started: 24 July 2026

3.1 Harvestable inflow and storage architecture

Two physically separate subsystems are modelled, reflecting the island's plumbing. Distributed cisterns receive only rooftop harvest,

$$I_{roof}(t) = C_{roof} \times \eta \times P(t) \times A_{roof} \quad (4)$$

with roof runoff coefficient $C_{roof} \approx 0.85$ and collection efficiency $\eta \approx 0.80$. The main system (reservoir + ponds + water bank, combined capacity 116,144 m³) receives the watershed runoff,

$$I_{run}(t) = C_{ws} \times P(t) \times A_{ws} + A_{res} \times P(t) \quad (5)$$

with weighted $C_{ws} = 0.31$ and $A_{ws} = 268{,}878$ m², and $A_{res} = 34{,}335$ m² the open-water surface of the reservoir and ponds (class W2, Table 1) that receives rainfall directly. Defining inflow as the water that actually reaches each store avoids conflating gross island rainfall with harvestable supply.

3.2 Two-subsystem monthly water balance with carry-over

Demand each month is met in order — cisterns (own rooftop water) first, then the main system, then groundwater, then imported PWA water — and each store carries over subject to its capacity:

$$S_{tank}(t) = \min\left\{V_{tank}, \max\left[0, S_{tank}(t-1) + I_{roof}(t) - Q_{tank}(t)\right]\right\} \quad (6)$$

$$S_{main}(t) = \min\left\{V_{main}, \max[0, S_{main}(t-1) + I_{run}(t) - Q_{main}(t)]\right\} \quad (7)$$

Any volume above capacity spills; cistern spill quantifies rooftop water lost because household tanks are small relative to wet-season inflow. The monthly shortfall that must be imported is

$$Def(t) = \max\left\{0, D(t) - Q_{tank}(t) - Q_{main}(t) - W_{gw}(t)\right\} \quad (8)$$

The model is run over the repeating annual cycle to a periodic steady state.

3.3 Supply performance: reliability–resilience–vulnerability

A month is satisfactory if it requires no import (Def = 0 after groundwater). Reliability is the satisfactory fraction of months, resilience the rate of recovery from failure, and vulnerability the mean shortfall during failures (Hashimoto et al., 1982):

$$Rel = \frac{1}{N}\sum_{t} 1[Def(t) = 0] \qquad Res = \frac{N_{f\to \mathrm{ok}}}{N_{\mathrm{fail}}} \qquad Vul = \overline{Def}(Def > 0) \quad (9)$$

This self-sufficiency criterion is appropriate for an island whose security is measured by independence from costly mainland imports.

3.4 Deterministic optimisation and the catchment–storage trade-off

For the mean year, capacity is sized by a mixed-integer linear program in which a binary y(t) marks an import month and $\Sigma\, y(t) \le (1 - R^*)N$ enforces a reliability target R^*. Decision variables are the additional catchment ΔA_{cat} (routed to the main

https://doi.org/10.5194/egusphere-2026-4005
Preprint. Discussion started: 24 July 2026

system), additional storage ΔV, the monthly withdrawals, groundwater and import. To keep the framework transferable across economies with different price levels, the objective minimises imported water rather than monetary cost,

$$\min \sum_{t} W_{ext}(t) \text{ subject to Eqs. (4 to 8)}, 0 \leq S \leq V + \Delta V, \sum_{t} y(t) \leq (1 - R^{*})N \tag{10}$$

and the catchment–storage trade-off is mapped by repeating the optimisation for a range of added storage. Reporting designs in physical units (catchment area, storage volume, import days) avoids dependence on site-specific unit costs; the economic choice along the trade-off is left to local prices.

In full, the program's decision variables are ΔA_{cat}, ΔV and, for each month t, the cistern and main withdrawals $Q_{tank}(t)$ and $Q_{main}(t)$, groundwater use $W_{gw}(t) \leq 1{,}440$ m³, import $W_{ext}(t)$, and a binary y(t) flagging an import month; the objective minimises $\sum_t W_{ext}(t)$. Constraints comprise the two carry-over mass balances (Eqs 6–7), the shortfall definition (Eq 8), the storage bounds $0 \leq S_{tank} \leq V_{tank}$ and $0 \leq S_{main} \leq V_{main} + \Delta V$, the groundwater and daily-import caps, the reliability constraint $\sum_t y(t) \leq (1 - R^{*})N$ with $R^{*} = 0.9$ and $N = 12$, and the big-M link $W_{ext}(t) \leq M \cdot y(t)$. The trade-off of Figure 8 is traced by solving this program over a grid of fixed ΔV and recording the minimum feasible ΔA_{cat}.

3.5 Stochastic rainfall generation and robust design

Because a single mean year cannot represent dry-year risk, a Monte-Carlo generator produces monthly rainfall that preserves the observed monthly means while imposing variability: each year is scaled by a lognormal annual factor (mean 1, inter-annual CV ≈ 0.20) and each month by an independent gamma multiplier (mean 1, CV ≈ 0.35). The realised annual CV is ≈0.24, with a 1-in-10 dry year near 860 mm. Robust capacities are sized on a continuous multi-year drought sequence — the lowest-rainfall decade from a long synthetic record — so that carry-over across consecutive dry years is captured; the first-stage capacities are common to all months while operations are month-specific over the 120-month horizon, with a sustainability constraint (end storage ≥ start storage). Each design is then evaluated out-of-sample by Monte-Carlo simulation over ≈1,450 independent years.

The Monte-Carlo sample size is justified by a convergence test (Table 8): the 95 % confidence half-width of the long-run reliability estimate falls below 0.01 beyond ≈500 years and is ≈0.007 at the ≈1,450 years used, so reported reliabilities are precise to better than one percentage point. The water-balance, optimisation and Monte-Carlo code is released (see Code and data availability).

3.6 Climate forcing and scenarios

Forcing uses a CMIP5 ensemble (HadGEM-AO, CanESM2, MPI-ESM-LR) downscaled by a cascade-forward artificial neural network. Rather than adopt one model a priori, the three members are first checked for downscaling skill and then screened for selection. The calibration and validation correlations between downscaled and observed variables are uniformly high (Table 4), confirming that every member is downscaled with acceptable skill; these correlations, however, are not the basis for choosing among models. Model selection for the design runs is instead made on annual-rainfall bias — the deviation of each

https://doi.org/10.5194/egusphere-2026-4005
Preprint. Discussion started: 24 July 2026

member's projected annual total from the observed 10-year mean (1,195.3 mm) — because it is the harvested water volume, not the day-to-day correlation, that governs the supply balance. Applying this criterion across all members and scenarios (Table 5) disqualifies MPI-ESM-LR, which overestimates annual rainfall by +108 % to +148 % and would grossly oversize the infrastructure. Both CanESM2 and HadGEM-AO fall within ±10 % under RCP4.5 (+6.3 % and −2.8 %, respectively); between them, HadGEM-AO is preferred for its dry-season fidelity — its downscaled hindcast of the 2012-2021 baseline decade reproduces the critical early-dry-season months (baseline-decade hindcast vs observed: February 24.9 vs 21.8 mm; March 23.9 vs 28.7 mm) and the monsoon peak, whereas CanESM2 carries a wet bias that overestimates July and underestimates January, the month our analysis identifies as the bottleneck. RCP4.5 is retained as the policy-relevant intermediate pathway; as a robustness check, CanESM2/RCP4.5 (the next-best member) was also run and left the qualitative conclusions unchanged. CMIP5/RCP is retained for consistency with Thailand's nationally adopted assessments and comparability with prior downscaled basin studies; migration to CMIP6/SSP is identified as future work. Three scenarios are evaluated: S1 current population and observed climate, S2 future population and historical climate, and S3 future population and the screened RCP4.5 climate.

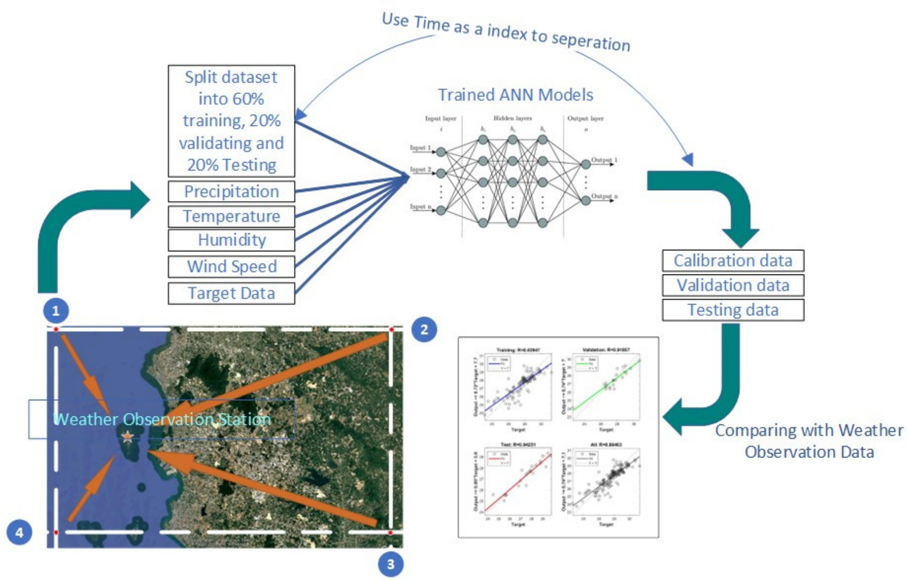

Figure 6: Overall Process to Climate Change Evaluation. Imagery © 2026 Airbus via Google Earth.

https://doi.org/10.5194/egusphere-2026-4005
Preprint. Discussion started: 24 July 2026

Table 4. Pearson Correlation Coefficients (*R*) in Each Parameter of Si Chang Island

Models	Parameter	Calibration			Validation		
		RCP2.6	RCP4.5	RCP8.5	RCP2.6	RCP4.5	RCP8.5
HadGEM-AO	Temperature	0.8603	0.8611	0.8637	0.8499	0.8340	0.8250
	Precipitation	0.8560	0.7981	0.7819	0.8800	0.7929	0.8196
	Humidity	0.7820	0.8173	0.7809	0.7738	0.8649	0.7847
	Wind Speed	0.7831	0.8207	0.8042	0.7965	0.8168	0.8007
CanESM2	Temperature	0.8526	0.8580	0.8495	0.8651	0.8279	0.8050
	Precipitation	0.8091	0.7970	0.8130	0.8447	0.8071	0.8021
	Humidity	0.8458	0.7849	0.7889	0.7951	0.8200	0.8668
	Wind Speed	0.7956	0.7995	0.7980	0.8350	0.8221	0.8337
MPI-ESM-LR	Temperature	0.8340	0.8557	0.8471	0.8098	0.8505	0.8438
	Precipitation	0.8030	0.7718	0.7894	0.8236	0.8596	0.8210
	Humidity	0.7970	0.7864	0.7854	0.7047	0.7024	0.7048
	Wind Speed	0.7836	0.7910	0.7879	0.8271	0.7908	0.8363

Table 5. Projected annual rainfall of each downscaled GCM by scenario, with deviation from the observed 10-year mean (1,195.3 mm); an asterisk (*) marks the retained RCP4.5 projections, which fall within the ±10 % engineering-acceptable band used for model selection.

Model	RCP2.6	RCP4.5	RCP8.5
CanESM2	1,381 (+15.5 %)	1,271 (+6.3 %)*	1,161 (−2.9 %)*
HadGEM-AO	997 (−16.6 %)	1,162 (−2.8 %)*	1,129 (−5.5 %)*
MPI-ESM-LR	2,485 (+108 %)	2,661 (+123 %)	2,966 (+148 %)

Future rainfall projections for Si Chang Island under the RCP 4.5 scenario using the HadGEM-AO model indicate that the month of January will become the most critical period for water availability. While the historical 10-year average for January is 56.8 mm, the 20-year projection (2026–2046) shows a sharp decline, averaging only 17.9 mm, representing a 68.5% reduction. This projected reduction is the most significant among all months and poses serious implications for early-year water stress (Figure 7).

Peak monsoon months (September and October) continue to show high rainfall, averaging 183.7 mm and 168.7 mm respectively. The months of December to March demonstrate a consistent pattern of low rainfall. Under the 2026–2046 projection, February averages 27.5 mm, and March 50.5 mm; both may be insufficient to maintain continuous supply without supplemental storage or alternative sources.

The projected annual average rainfall of 1,161.8 mm remains close to the historical value of 1,195.3 mm, suggesting that while total volume may remain stable, temporal distribution will shift toward greater dry-season deficits. The diminished rainfall in January not only increases dependency on stored or imported water but also underscores the importance of precisely timed reservoir operations, demand-side management, and diversification of supply sources (Figure 7). Overall, these findings

https://doi.org/10.5194/egusphere-2026-4005
Preprint. Discussion started: 24 July 2026

indicate that climate-resilient planning must prioritize bridging shortfalls in January and the broader December–March period, which will increasingly become the bottleneck for year-round water security on small islands like Si Chang Island.

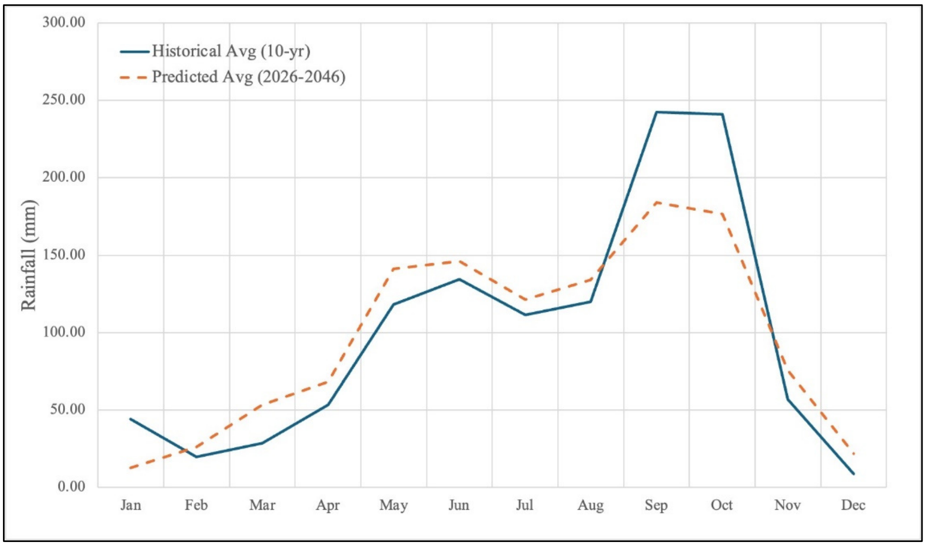

Figure 7: Historical 10-year *vs* Projected Average Rainfalls under RCP4.5, HadGEM-AO model

4 Results

4.1 Demand, harvestable supply and the structural balance

At present the island must supply about 328,244 m³ yr⁻¹ (Table 3). Against this, the two harvestable inputs are rooftop harvest, with an annual potential of $C_{roof} \times \eta \times P \times A_{roof} \approx 0.85 \times 0.80 \times 1.195\ \mathrm{m} \times 2.45 \times 10^5\ \mathrm{m}^2 \approx 199{,}120\ \mathrm{m}^3$, and watershed runoff to the reservoir ≈ 140,020 m^3; sustainable groundwater adds at most 17,280 $\mathrm{m}^3\ \mathrm{yr}^{-1}$. Rooftop harvest alone therefore exceeds reservoir runoff, making distributed harvesting — not the reservoir — the dominant freshwater source. Under projected demand (402,852 $\mathrm{m}^3\ \mathrm{yr}^{-1}$) the three local inputs sum to 356,420 $\mathrm{m}^3\ \mathrm{yr}^{-1}$, leaving a structural annual deficit of 46,432 $\mathrm{m}^3\ \mathrm{yr}^{-1}$ that no redistribution of storage can remove.

4.2 Baseline reliability

Routing these inputs through the two-subsystem balance (Table 6) shows that the present system is reliable (reliability 0.92, resilience 1.00) but cistern-limited: about 25,000 m^3 of rooftop water spills each year because the 5,650 m^3 of household cisterns are too small to hold the wet-season surplus, and only ≈9 import-days per year are needed. Under projected demand

https://doi.org/10.5194/egusphere-2026-4005
Preprint. Discussion started: 24 July 2026

reliability falls to 0.75 with three failure months, resilience drops to 0.33, vulnerability nearly doubles, and imports rise to ≈49 days. The deterioration is driven by the structural deficit of Section 4.1, not by a lack of storage.

Table 6. Baseline water balance and RRV under the two-subsystem model

Scenario	Rooftop used ($m^3\ yr^{-1}$)	Rooftop spill ($m^3\ yr^{-1}$)	Main system ($m^3\ yr^{-1}$)	Import (d yr^{-1})	Reliability	Resilience	Vulnerability (m^3)
Current (P_{tot} 8,289)	173,987	25,134	140,020	9	0.92	1.00	12,798
Future (P_{tot} 10,173)	185,291	13,830	140,020	49	0.75	0.33	24,407

4.3 Deterministic optimisation

Because the future deficit is structural, both storage-only programs — expanding cisterns or main storage with no new catchment — are infeasible for reliability ≥0.9: storage redistributes water in time but cannot create it. Feasible designs must add harvestable catchment, and the amount needed trades off against added storage (Figure 8). With no additional storage, reaching reliability ≥0.9 on the mean year requires ≈206,500 m² of extra catchment to cover the worst dry month directly; adding 20,000 m³ of storage to buffer the dry season lowers the requirement to ≈93,600 m², beyond which the curve flattens. The trade-off is reported in physical units precisely because the economic balance between building catchment and building storage depends on local prices, which differ widely between settings.

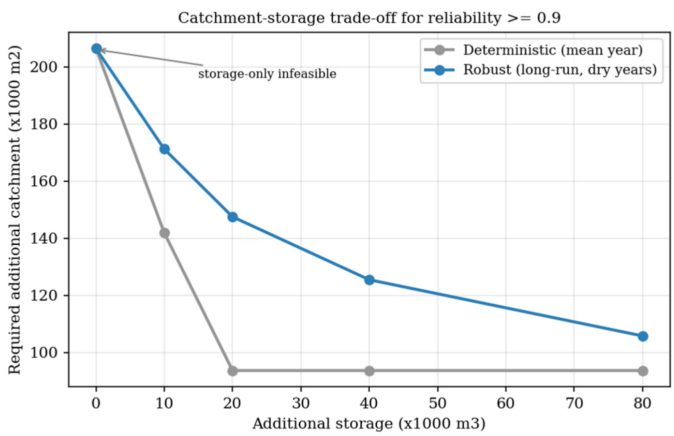

Figure 8. Catchment–storage trade-off for reliability ≥0.9.

https://doi.org/10.5194/egusphere-2026-4005
Preprint. Discussion started: 24 July 2026

4.4 Stochastic robustness

Evaluated across ≈1,450 simulated years, a design sized on the mean year is far less reliable than it appears. For example, with 20,000 m³ of added storage the mean-year optimum of ≈93,600 m² of catchment — which meets reliability ≥0.9 on the mean year — achieves a long-run reliability of only 0.83, fails the 0.9 target in most years, and is drawn down completely in the driest years. Sizing on a multi-year drought instead, the same 20,000 m³ of storage requires ≈147,400 m² of catchment — about 57 % more (Table 7) — to deliver a long-run reliability of 0.90, and the full robust trade-off (Figure 8, upper curve) lies consistently above the deterministic one. The gap between the two curves is the previously hidden cost of hydrological variability, and it explains why deterministic island-supply assessments can be over-optimistic. The seasonal storage dynamics underlying this robust design are illustrated in Figure 9, which traces the main-system storage over a representative operating year: the reservoir fills through the September–October monsoon peak to near its 136,144 m³ capacity (the 116,144 m³ base plus the 20,000 m³ of added storage), then draws down progressively through the December–April dry season to a minimum in April before the wet season resumes, confirming that carry-over from the wet season is what sustains dry-season supply. The contrast in long-run performance between the two designs is summarised in Figure 10, which shows that the mean-year design fails the 0.9 target in most years whereas the robust design meets it.

Table 7. Mean-year (deterministic) versus robust design at a fixed added storage of 20,000 m³, evaluated out-of-sample by Monte-Carlo simulation (≈1,450 years).

Design basis	ΔA_{cat} (m²)	ΔV (m³)	Long-run reliability	Import (d yr⁻¹)
Mean-year (deterministic)	93,600	20,000	0.83	≈22
Robust (dry-year)	147,400	20,000	0.90	≈11

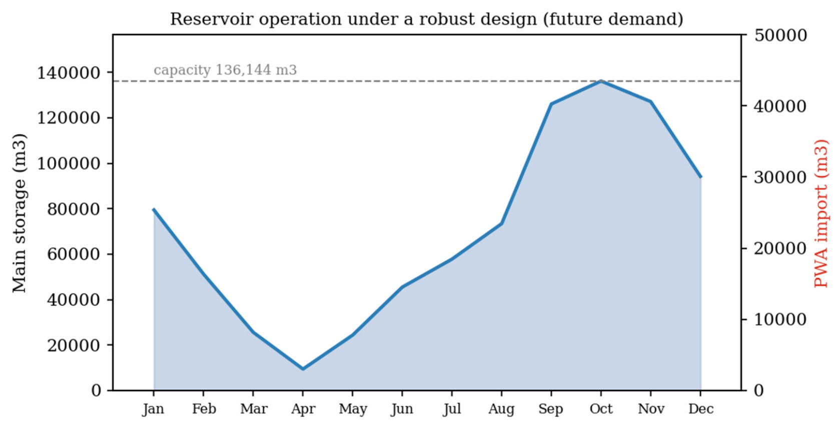

Figure 9. Reservoir operation over a representative year under a robust design.

https://doi.org/10.5194/egusphere-2026-4005
Preprint. Discussion started: 24 July 2026

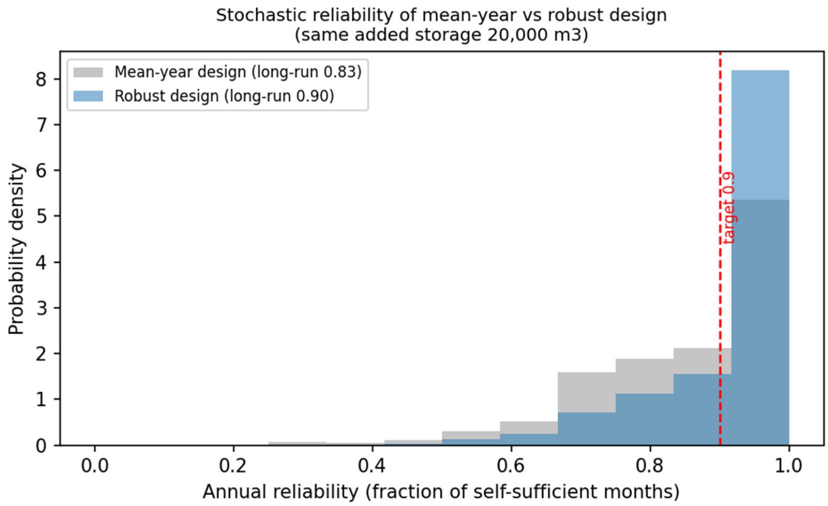

Figure 10. Monte-Carlo distribution of annual reliability for the mean-year and robust designs at the same added storage.

Table 8. Monte-Carlo convergence of the long-run reliability estimate for the robust design (147,400 m², +20,000 m³): the 95 % confidence half-width of the long-run reliability estimate falls below 0.01 by ≈1,000 years (0.011 at 500 years, 0.008 at 1,000) and is ≈0.007 at the ≈1,450 years used

N (years)	100	250	500	1,000	1,450	2,000	3,000	5,000
Long-run reliability	0.911	0.896	0.907	0.905	0.902	0.908	0.899	0.898
95 % CI half-width	0.047	0.016	0.011	0.008	0.007	0.006	0.005	0.004

4.5 Sensitivity and uncertainty analysis

Because several inputs are estimated rather than directly measured, we tested how the two headline results — the structural supply deficit and the drought-robust catchment requirement — respond to ±10 % and ±20 % variation in the five most uncertain parameters: connected roof area, watershed runoff coefficient, transient-tourism demand, per-capita use and sustainable groundwater yield, each varied one at a time (Figure 11).

https://doi.org/10.5194/egusphere-2026-4005
Preprint. Discussion started: 24 July 2026

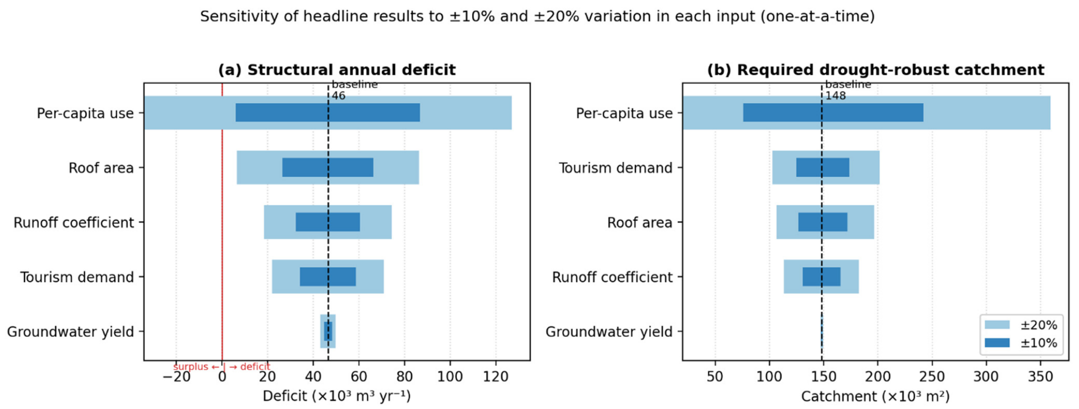

Figure 11. Sensitivity of the structural deficit (a) and the required drought-robust catchment (b) to ±10 % (dark) and ±20 % (light) variation in each input (one-at-a-time); dashed line marks the baseline.

The structural annual deficit (Table 9) stays positive — the island remains supply- rather than storage-limited — under every ±10 % perturbation and under all ±20 % perturbations except a −20 % reduction in per-capita use, the only case returning a small surplus. Per-capita demand is therefore the pivotal assumption; roof area, runoff and tourism demand are moderately influential, and groundwater yield negligible.

Table 9. Sensitivity of the future structural annual deficit ($m^3\ yr^{-1}$; baseline 46,432) to ±10 % and ±20 % variation in each input. The island is supply-limited wherever the deficit exceeds zero.

Parameter	−20 %	−10 %	+10 %	+20 %
Per-capita use	−34,138	6,147	86,717	127,002
Roof area	86,256	66,344	26,520	6,608
Runoff coefficient	74,436	60,434	32,430	18,428
Tourism demand	22,025	34,228	58,636	70,839
Groundwater yield	49,888	48,160	44,704	42,976

The required drought-robust catchment (Table 10) confirms per-capita use as the dominant control, though the intermediate ordering shifts: tourism demand outranks roof area and runoff for the catchment requirement, whereas it ranks below them for the deficit (Table 9). Both analyses identify metered per-capita consumption and a visitor-demand survey as the highest-value data for reducing design uncertainty, consistent with the plausibility check in Sect. 4.7.

Table 10. Sensitivity of the required drought-robust catchment (m^2 at +20,000 m^3 storage; baseline ≈148,100) to ±10 % and ±20 % variation in each input, ranked most to least influential.

Parameter	−20 %	−10 %	+10 %	+20 %
Per-capita use	20,000	76,000	241,900	359,200

https://doi.org/10.5194/egusphere-2026-4005
Preprint. Discussion started: 24 July 2026

Parameter	−20 %	−10 %	+10 %	+20 %
Tourism demand	103,000	124,700	173,600	201,700
Roof area	196,400	171,700	126,400	106,600
Runoff coefficient	182,600	165,300	130,800	113,600
Groundwater yield	149,600	148,700	147,600	147,000

The sensitivity baseline (≈148,100 m²) is the robust optimum re-evaluated on the independent Monte-Carlo sample used for the one-at-a-time analysis. It differs from the 147,400 m² reported in Table 7 only through Monte-Carlo sampling variability (<0.5 %): the two values are the same design optimum estimated from different finite stochastic samples, not different quantities. All perturbations in Table 10 are referenced to this internally consistent baseline, so the relative sensitivities are unaffected.

4.6 Effect of evaporation and seasonal tourism

Two processes omitted from the core balance were added and evaluated on the robust design (147,400 m², +20,000 m³; Figure 12 and Table 11). Open-water evaporation from the reservoir–pond surface (net ≈1,300 mm yr⁻¹) was applied under a conservative constant full-surface treatment and a realistic level-dependent treatment in which the evaporating area shrinks with storage volume. The level-dependent treatment lowers long-run reliability from 0.90 to ≈0.85 (≈19,500 m³ yr⁻¹ lost), the constant-area upper bound to ≈0.79; because loss peaks in November–January when the reservoir is full — the water carried into the dry season — even the milder estimate erodes early-dry-season storage. Concentrating tourism into the cool-season and Songkran peaks (raising mean dry-season demand by ≈11 % and April demand by ≈23 %) independently lowers reliability to ≈0.86, as the demand peak meets the supply trough. Acting together the two processes give ≈0.82, and restoring 0.90 requires expanding the catchment to ≈258,000 m² — about 75 % above the baseline design. Both refinements reinforce, rather than overturn, the supply-limited finding and confirm the reported capacities as conservative lower bounds.

Table 11. Long-run reliability of the robust design under open-water evaporation and seasonal (peak) tourism, relative to the core balance (0.90).

Scenario	Uniform tourism	Seasonal (peak) tourism
No evaporation	0.90	0.86
Level-dependent evaporation (realistic)	0.85	0.82
Constant-area evaporation (upper bound)	0.79	0.78

https://doi.org/10.5194/egusphere-2026-4005
Preprint. Discussion started: 24 July 2026

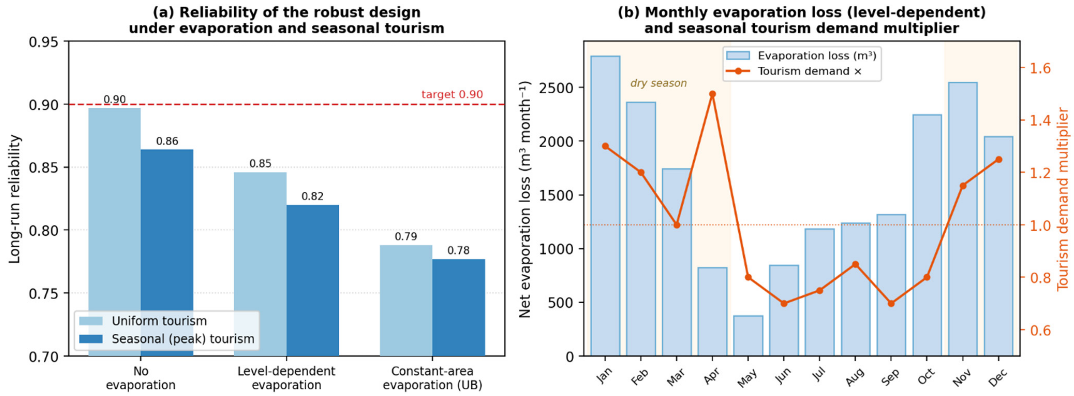

Figure 12. (a) Long-run reliability of the robust design under evaporation and seasonal tourism; (b) monthly net evaporation loss (level-dependent) and the seasonal tourism-demand multiplier.

4.7 Plausibility check against field evidence

In the absence of a continuous metered record, the modelled behaviour is checked against independent field evidence. Si Chang was declared Thailand's first drought-disaster district of 2023 (27 March 2023), during the December–April dry season that the model identifies as the reliability bottleneck (Office of the National Water Resources, 2023). Emergency supply is delivered by barge from the mainland — reported at about 2,000 m³ per delivery, sufficient for roughly five days (≈400 m³ d⁻¹) — corroborating the model's treatment of imported water as a costly, capacity-limited contingency; at acute shortage households reportedly bought water at up to 250 THB per unit (Ministry of Interior, 2024). The reported service base of about 400 of 2,200 households is consistent with the registered count (2,270) (Department of Provincial Administration, Thailand, 2024) used here, and provincial mitigation — additional water banks, reservoir rehabilitation and a proposed sub-sea pipeline from Si Racha — mirrors the diversified storage-and-import architecture represented in the model. Local assessments further confirm that the island is affected by dry-season shortage essentially every year (Srisuk et al., 2022). These correspondences provide an observational plausibility check; a continuous metered record remains the priority validation dataset (Sect. 6).

5 Implications

5.1 Principal implications

Three implications follow directly from the results. Methodologically, deterministic mean-climate optimisation is optimistically biased for island water security: at a fixed added storage it understates the required catchment by roughly 57 %, and a design that appears to meet a 0.9 reliability target on the mean year delivers only about 0.83 over the long run. Reliability claims for island systems should therefore be made on a stochastic, multi-year basis. In engineering terms, once demand grows

https://doi.org/10.5194/egusphere-2026-4005
Preprint. Discussion started: 24 July 2026

the binding constraint is supply rather than storage: the structural annual deficit cannot be removed by any redistribution of water in time, so additional harvestable catchment — not larger cisterns or reservoirs alone — is the decisive lever. Economically, because barged imports impose a recurring burden, augmenting local catchment is attractive wherever import costs are high, although the precise balance between investing in catchment and in storage is site-specific and is deliberately left to local prices along the trade-off frontier (Figure 8).

5.2 Implementation pathway for Si Chang Island

The catchment expansion implied by the robust design need not be greenfield construction. The island already carries extensive impervious roofs — 0.42 km^2 of industrial and 0.16 km^2 of institutional buildings (Table 1) — that are largely unconnected to the supply system; routing a quarter to a half of this area to the reservoir–pond network through gutters, downpipes and short conveyance lines would meet the robust target. Because the catchment–storage trade-off is continuous (Figure 8), implementation can be incremental and adaptive: the largest roofs nearest the reservoir can be connected first to minimise conveyance, with further connections staged as demand grows and as monitored reliability indicates, so the system moves along the frontier rather than committing to a single large capital scheme.

Three accompanying measures matter for delivery. First, runoff from industrial and institutional surfaces requires first-flush diversion and basic treatment before entering the potable reservoir, together with source control on the contributing roofs, so that catchment expansion does not import contamination. Second, a modest storage complement is valuable: Figure 8 shows that roughly 20,000 m^3 of added buffering — achievable by upgrading the existing pond and water-bank system, or in time through managed aquifer recharge — substantially lowers the catchment that must be built. Third, at the household scale the present loss of about 25,000 $m^3\ yr^{-1}$ of rooftop water to cistern spill (Table 6) indicates that even small increases in distributed cistern volume would recover usable water and complement the main-system expansion.

Finally, the robust, stochastic framing argues for adaptive management rather than a one-off design. Metering of supply and demand, reservoir-level telemetry, and dry-season demand management — including for the tourism sector that drives the seasonal peak — would allow the operating policy and the chosen design point to be revised as climate and demand evolve, and would generate the validation data, metered consumption and reservoir levels, that the present study lacks. Embedding such monitoring converts a static design into a living plan able to track the moving target that climate change represents.

5.3 Implications for small islands under climate change

Several findings are likely to generalise to other rainfall-and-reservoir small islands. The most consequential is that, under demand growth and a drier or more variable dry season, the binding constraint shifts from storage to supply. Island adaptation planning frequently defaults to enlarging reservoirs or cisterns, yet where annual harvestable inflow falls below annual demand no amount of storage can close the gap. Recognising this reframes adaptation priorities towards augmenting harvestable sources — connected catchment, managed recharge, and, where unavoidable, desalination — and towards demand management, rather than storage alone (Global Center on Adaptation, 2025; Parker et al., 2023).

https://doi.org/10.5194/egusphere-2026-4005
Preprint. Discussion started: 24 July 2026

The optimism bias of mean-climate design is a second, general caution. Adaptation infrastructure sized on average or single-scenario rainfall will under-deliver reliability, and the shortfall widens precisely as climate change increases inter-annual variability and the frequency of the multi-year droughts that drive island-supply failures (Holmes et al., 2022). Robust, multi-year stochastic sizing — and the explicit screening of climate scenarios for engineering use adopted here — is therefore not a refinement but a prerequisite for credible island adaptation, and it becomes more important, not less, under stronger warming.

A third lesson concerns accounting. Many islands appear water-secure in aggregate yet fail in practice because stocks and fluxes are conflated and self-sufficiency is overstated (Global Center on Adaptation, 2025); the physically consistent, two-subsystem accounting used here exposes the true balance and the dominance of distributed rooftop harvesting. That dominance is itself encouraging, since decentralised harvesting is low-carbon relative to desalination, has no single point of failure, and scales with the building stock — provided it is sized for drought rather than for the mean. The framework transfers readily to other small islands, whereas the specific capacities reported here are particular to Si Chang Island and would be re-derived from local land use, rainfall and demand elsewhere.

6 Limitations

Several limitations qualify these results, although none reverses the central conclusions. On the climate side, the stochastic generator is stationary about the RCP4.5 monthly means: it reproduces realistic inter-annual and multi-year variability but not trends in that variability or in dry-spell structure. Because climate change is expected to widen variability rather than narrow it, this assumption is conservative — it most likely understates, not overstates, the catchment required for robustness — and a CMIP6/SSP forcing with non-stationary statistics is the natural next step. Two further simplifications act in the same direction. The core water balance omits open-water evaporation and seepage as an explicit monthly loss; their magnitude is quantified in Sect. 4.6, where including evaporation and a seasonal-tourism profile lowers reliability but confirms the reported capacities as conservative lower bounds. Likewise, evaluation uses a single rule-based operating policy; a closed-loop or stochastic-dynamic policy could extract more reliability from a given capacity, meaning the reported designs are an upper bound on the infrastructure needed rather than a floor. A related point concerns the rainfall series used in the balance. The design runs are driven by the historical 10-year monthly means rather than by the RCP4.5 projections, and are therefore a deliberately conservative baseline: the projections indicate a marked drying of the early dry season — January falling by about 68 %, from 56.8 to 17.9 mm (Sect. 3.6) — which would deepen the dry-season deficit and so raise, not lower, the harvestable catchment required for a given reliability. The capacities reported here should thus be read as lower bounds, and sizing directly on the projected series is a priority for the next iteration.

The remaining limitations concern data rather than model structure and define the priorities for validation. Connected roof area rests on a household-and-imagery estimate bracketed between independent lower and upper bounds; direct GIS footprint digitisation, together with metered consumption and reservoir-level records, would tighten this central input and allow the modelled reliabilities to be validated against observed import behaviour. The demand parameters — visitor stay lengths, the

https://doi.org/10.5194/egusphere-2026-4005
Preprint. Discussion started: 24 July 2026

transient-labour fraction and per-capita use — derive from survey values and warrant a formal sensitivity analysis, since they scale the demand that the system must meet. These are measurement refinements rather than structural gaps, and the qualitative results — the dominance of rooftop harvesting, the structural supply deficit, and the optimism of mean-climate design — are robust to plausible variation in them.

7 Conclusions

We presented an integrated assessment of dry-season water-scarcity risk for a tourism-exposed, fractured-rock island, combining a measured harvestable-catchment estimate, a two-subsystem monthly water balance with storage carry-over, an embedded tourism-demand term, RRV performance metrics under a downscaled climate ensemble, and a mixed-integer optimisation extended to a robust, stochastic design.

Three findings stand out. First, when storage stocks and inflow fluxes are separated and routed through their actual plumbing, rooftop harvesting — not the reservoir — is the dominant freshwater source, and the present system is reliable but constrained by small distributed cistern capacity. Second, under projected demand the island faces a structural annual supply deficit, making it supply- rather than storage-limited: additional storage alone cannot secure reliability, which instead requires expanding harvestable catchment, plausibly by connecting existing industrial and institutional roofs. Third, optimisation on mean rainfall is optimistically biased — an apparently adequate design fails in most years once realistic inter-annual and multi-year-drought variability is imposed — so drought-robust sizing, which here needs about 57 % more catchment at a given storage, is essential.

For Si Chang Island, the practical recommendation is to expand and connect rooftop or engineered catchment to the existing reservoir under a drought-robust design target, rather than to enlarge household cisterns alone. Future work should adopt CMIP6/SSP forcing, add open-water evaporation and managed aquifer recharge, validate against metered consumption and reservoir-level records, and apply local unit costs to select the economically preferred point on the catchment–storage trade-off.

Code and data availability

The land-use layer, rainfall records and storage inventory, together with the Python code for the water balance, optimisation and Monte-Carlo analysis, are available from the corresponding author on reasonable request and will be deposited in a public repository with a DOI upon acceptance.

https://doi.org/10.5194/egusphere-2026-4005
Preprint. Discussion started: 24 July 2026

Author contributions

Seeboonruang, U. designed the research framework, supervised data analysis, acquired the funding and reviewed the manuscript. Tanachaichoksirikun, P. developed the optimization model, performed simulations, and wrote the original manuscript. Chulkaivalsucharit, V. contributed to climate downscaling analysis and data visualization. Sirikaew, U. collected hydrological and infrastructure data and assisted in GIS mapping. Prasitkumpein, M. contributed to interpretation of policy implications and water governance frameworks. Srisuk, J. conducted field surveys, supported integration of socio-economic datasets, performed simulations, and wrote the original manuscript. Chen, W. collaborated with funding, reviewed and edited the manuscript. All authors discussed results, revised the manuscript, and approved the final version.

Competing interests

The authors declare that they have no conflict of interest.

Acknowledgements

The authors gratefully acknowledge the KMITL, School of Engineering and Provincial Waterworks Authority (PWA) for providing relevant data and valuable on-site assistance, which significantly contributed to the fieldwork and system assessment conducted on Si Chang Island. During the preparation of this manuscript/study, the authors used Claude.ai (Opus 4.8) to assist with language refinement, structural organization, and clarity improvement of the manuscript. All technical content, modelling procedures, data analysis, and scientific interpretations were developed and verified by the authors. The authors take full responsibility for the content of the publication.

Financial support

This research was financially supported under the Memorandum of Understanding (MoU) research collaboration between National Taipei University of Technology, Taiwan, and King Mongkut's Institute of Technology Ladkrabang, Thailand (Grant No. KREF156502). The authors sincerely appreciate this financial sponsorship.

References

Asefa, T., Clayton, J., Adams, A., and Anderson, D.: Performance evaluation of a water resources system under varying climatic conditions: Reliability, Resilience, Vulnerability and beyond, J. Hydrol., 508, 53–65, https://doi.org/10.1016/j.jhydrol.2013.10.043, 2014.

Ault, T.: Water resources: Island water stress, Nat. Clim. Chang., 6, 1062–1063, https://doi.org/10.1038/nclimate3171, 2016.

Beh, E. H. Y., Zheng, F., Dandy, G. C., Maier, H. R., and Kapelan, Z.: Robust optimization of water infrastructure planning under deep uncertainty using metamodels, Environ. Model. Softw., 93, 92–105, https://doi.org/10.1016/j.envsoft.2017.03.013, 2017.

Birawida, A. B., Ibrahim, E., Mallongi, A., Rasyidi, A. A. Al, Thamrin, Y., and Gunawan, N. A.: Clean water supply vulnerability model for improving the quality of public health (environmental health perspective): A case in Spermonde islands, Makassar Indonesia, Gac. Sanit., 35, S601–S603, https://doi.org/10.1016/j.gaceta.2021.10.095, 2021.

Chen, H. and Tang, R.: From vulnerability to vitality: Climate change as a catalyst for economic transformation in small island developing states, Dev. Sustain. Econ. Financ., 1, 100005, https://doi.org/10.1016/j.dsef.2024.100005, 2024.

Dash, S. S., Sahoo, B., and Raghuwanshi, N. S.: An integrated reservoir operation framework for enhanced water resources planning, Sci. Rep., 13, 1–22, https://doi.org/10.1038/s41598-023-49107-z, 2023.

Department of Provincial Administration, Thailand: Population in Chonburi, 2024.

Fiaz, A., Rahman, G., and Kwon, H.-H.: Impacts of climate change on the South Asian monsoon: A comprehensive review of its variability and future projections, J. Hydro-environment Res., 59, 100654, https://doi.org/10.1016/j.jher.2025.100654, 2025.

Global Center on Adaptation: Rethinking Water Management for a Changing Climate in SIDS: https://gca.org/rethinking-water-management-for-a-changing-climate-in-sids/, (last access: 30 June 2026), 2025.

Gössling, S.: The consequences of tourism for sustainable water use on a tropical island: Zanzibar, Tanzania, J. Environ. Manage., 61, 179–191, https://doi.org/10.1006/jema.2000.0403, 2001.

Gössling, S., Peeters, P., Hall, C. M., Ceron, J.-P., Dubois, G., Lehmann, L. V., and Scott, D.: Tourism and water use: Supply, demand, and security. An international review, Tour. Manag., 33, 1–15, https://doi.org/10.1016/j.tourman.2011.03.015, 2012.

Guo, Y., Yu, X., Xu, Y. P., Wang, G., Xie, J., and Gu, H.: A comparative assessment of CMIP5 and CMIP6 in hydrological responses of the Yellow River Basin, China, Hydrol. Res., 53, 867–891, https://doi.org/10.2166/nh.2022.001, 2022.

Haider, S., Masood, M. U., Rashid, M., Ali, T., Pande, C. B., Alshehri, F., and Elkhrachy, I.: Assessment of rainwater harvesting potential for urban area under climate and land use changes using geo-informatics technology, Urban Clim., 52, 101721, https://doi.org/10.1016/j.uclim.2023.101721, 2023.

Hashimoto, T., Stedinger, J. R., and Loucks, D. P.: Reliability, resiliency, and vulnerability criteria for water resource system performance evaluation, Water Resour. Res., 18, 14–20, https://doi.org/10.1029/WR018i001p00014, 1982.

Herman, J. D., Reed, P. M., Zeff, H. B., and Characklis, G. W.: How Should Robustness Be Defined for Water Systems Planning under Change?, J. Water Resour. Plan. Manag., 141, 1–14, https://doi.org/10.1061/(asce)wr.1943-5452.0000509, 2015.

Holding, S. and Allen, D. M.: Risk to water security for small islands: an assessment framework and application, Reg. Environ. Chang., 16, 827–839, https://doi.org/10.1007/s10113-015-0794-1, 2016.

Holmes, R. N., Mayer, A., Gutzler, D. S., and Chavira, L. G.: Assessing the Effects of Climate Change on Middle Rio Grande Surface Water Supplies Using a Simple Water Balance Reservoir Model, Earth Interact., 26, 168–179,

https://doi.org/10.5194/egusphere-2026-4005
Preprint. Discussion started: 24 July 2026

https://doi.org/10.1175/EI-D-21-0025.1, 2022.

Imig, A., Welsh, K., Klausner, S., Hotta, C. I., McKenzie, Z., Perosa, F., Stephens, M., Turner, A., Thomas, J., Chaves, H. M. L., Bowen-O′Connor, C., Moxey, A., Dokou, Z., and Rein, A.: Climate change resilience of freshwater supply on small islands: Research gaps and strategies for a case study in Grand Bahama, J. Hydrol. Reg. Stud., 59, 102430, https://doi.org/10.1016/j.ejrh.2025.102430, 2025.

Intergovernmental Panel on Climate Change: Regional fact sheet - Small Islands, Climate change 2021: the physical science basis, 10–11 pp., 2021.

Intergovernmental Panel on Climate Change: Climate Change 2022 – Impacts, Adaptation and Vulnerability, Cambridge University Press, 3068 pp., https://doi.org/10.1017/9781009325844, 2023.

Mashhadi Ali, A., Shafiee, M. E., and Berglund, E. Z.: Agent-based modeling to simulate the dynamics of urban water supply: Climate, population growth, and water shortages, Sustain. Cities Soc., 28, 420–434, https://doi.org/10.1016/j.scs.2016.10.001, 2017.

Ministry of Interior (MOI): Progress on the royal-initiative project to resolve the water shortage on Ko Sichang (in Thai), Government Public Relations Department, https://www.prd.go.th/th/content/category/detail/id/39/iid/321801, last access: 30 June 2026, 2024.

Mirzaei, M., Shirmohammadi, A., Ruiz-barradas, A., and Olson, L. J.: Urban Climate Climate change effects on the spatial and temporal distribution of extreme precipitation in the Mid-Atlantic region, Urban Clim., 61, 102382, https://doi.org/10.1016/j.uclim.2025.102382, 2025.

Nusara, P.: New normal of tourists towards tourism on Koh Sichang under the preventive measures and surveillance of COVID-19 infection (in Thai), Burapha University, 142 pp., 2021.

Office of the National Water Resources (ONWR): Ko Sichang declared the first drought-disaster district of 2023, Chon Buri (in Thai), https://www.thaipost.net/general-news/353918/, last access: 30 June 2026, 2023.

Okoye, C. O., Solyali, O., and Akintuı, B.: Optimal sizing of storage tanks in domestic rainwater harvesting systems: A linear programming approach, Resour. Conserv. Recycl., 104, 131–140, https://doi.org/10.1016/j.resconrec.2015.08.015, 2015.

Ortiz-Partida, J. P., Kahil, T., Ermolieva, T., Ermoliev, Y., Lane, B., Sandoval-Solis, S., and Wada, Y.: A Two-Stage Stochastic Optimization for Robust Operation of Multipurpose Reservoirs, Water Resour. Manag., 33, 3815–3830, https://doi.org/10.1007/s11269-019-02337-1, 2019.

Parker, S. Y., Parchment, K. F., and Gordon-Strachan, G. M.: The burden of water insecurity: a review of the challenges to water resource management and connected health risks associated with water stress in small island developing states, J. Water Clim. Chang., 14, 4404–4423, https://doi.org/10.2166/wcc.2023.239, 2023.

Pérez, D. M. G., Martín, J. M. M., Martínez, J. M. G., and Sáez-Fernández, F. J.: An analysis of the cost of water supply linked to the tourism industry. An application to the case of the Island of Ibiza in Spain, Water (Switzerland), 12, https://doi.org/10.3390/w12072006, 2020.

Sealey, K. S.: Assessing coastal vulnerability and climate resilience for Caribbean small island states using ecological

https://doi.org/10.5194/egusphere-2026-4005
Preprint. Discussion started: 24 July 2026

principles, Int. J. Disaster Risk Reduct., 105, 104410, https://doi.org/10.1016/j.ijdrr.2024.104410, 2024.

Seeboonruang, U., Horpeancharoen, W., Sirikaew, U., Tanachaichoksirikun, P., and Chulkaivalsucharit, V.: Identifying Water Source Locations on a Data-Limited Small Island Using GIS and the Factor Index Method, Water Resour. Manag., 40, 336, https://doi.org/10.1007/s11269-026-04739-4, 2026.

Semaan, M., Day, S. D., Garvin, M., Ramakrishnan, N., and Pearce, A.: Optimal sizing of rainwater harvesting systems for domestic water usages: A systematic literature review, Resour. Conserv. Recycl. X, 6, 100033, https://doi.org/10.1016/j.rcrx.2020.100033, 2020.

Srisuk, J., Tanachaichoksirikun, P., and Seeboonruang, U.: A Study of Water Quality for Consumption of Si-Chang Island with Geographic Information System (in Thai), in: 27th National Convention on Civil Engineering (NCCE27), 2022.

Srisuk, J., Tanachaichoksirikun, P., Sirikaew, U., and Seeboonruang, U.: Expected Groundwater Development and Water Security in Deficit Small Tourism Island, Int. J. GEOMATE, 30, 123–130, https://doi.org/10.21660/2026.137.g15285, 2026.

Tanachaichoksirikun, P.: Modelling Water Distribution Strategies for a Data-Limited Small Island Using EPANET: Technical and Policy Insights from Si Chang Island, Thailand, Water (Switzerland), 18, https://doi.org/10.3390/w18101166, 2026.

Thai Meteorological Department (TMD): Information Service Unit (personal contact), 2021.

Thomas, T. H. and Martinson, D. B.: Roofwater harvesting: a handbook for practitioners, 156 pp., 2007.

White, I. and Falkland, T.: Management of freshwater lenses on small Pacific islands, Hydrogeol. J., 18, 227–246, https://doi.org/10.1007/s10040-009-0525-0, 2010.

Wohl, E., Barros, A., Brunsell, N., Chappell, N. A., Coe, M., Giambelluca, T., Goldsmith, S., Harmon, R., Hendrickx, J. M. H., Juvik, J., McDonnell, J., and Ogden, F.: The hydrology of the humid tropics, Nat. Clim. Chang., 2, 655–662, https://doi.org/10.1038/nclimate1556, 2012.